LPV and Nonlinear-based control of an Autonomous Quadcopter under variations of mass and moment of inertia

The Hung Pham, Dalil Ichalal, Saïd Mammar

LPV and Nonlinear-based control of an Autonomous Quadcopter under variations of mass and moment of inertia ⋆

The Hung PHAM * **Dalil ICHALAL** ** **Said MAMMAR** ***
IBISC, Univ Evry, Université Paris Saclay, 40, rue de Pelvoux, Evry, France.

* *(e-mail: thehung.pham@univ-evry.fr, thehungpham83@gmail.com)*
** *(e-mail: dalil.ichalal@univ-evry.fr)*
*** *(e-mail: said.mammar@univ-evry.fr)*

Abstract: This paper presents a hybrid robust control strategy to solve the trajectory tracking function of a quadcopter with time-varying mass. In the context of this paper, two ways of changing the mass of a quadcopter are considered. The first one involves a gradual continuous reduction of the mass throughout the flying time, and the second involves an abrupt change at some point during the flight. Besides the change of the mass, the moments of inertia with respect to the three axes are also changing. These moments of inertia are recalculated in real-time according to the mass changes.
The quadcopter model is separated into two subsystems: rotational and translational. The rotational subsystem contains several time-varying parameters, such as the mass, the moments of inertia, and the speed of the rotor. It can be considered as a quasi-Linear Parameter Varying (LPV) system. An LPV H_∞ controller has been designed to stabilize the orientation actuator's dynamic. To ensure that the quadcopter follows the pre-defined trajectory, a combination of Integral Backstepping and Proportional Derivative (PD) controllers are used for the translational subsystem.
The efficiency and robustness of the proposed cascaded controller with disturbances, noises, and model parameters uncertainties have been tested in MATLAB.

Keywords: UAV, Quadcopter, Linear Parameter Varying, Backstepping, Proportional Integral Derivative, Linear Matrix Inequality, Robust Control, H_∞-Optimal control

1. INTRODUCTION

The quadrotor is a type of aircraft, which uses four lifting forces generated by four symmetrically fixed motors around its center. By controlling the four lifts, the quadrotor is able to hover and move without the complex system of linkages and blade elements commonly found in standard single rotor vehicles. Due to its flexibility, Vertical Take-Off and Landing (VTOL) is made relatively affordable for development and application costs Zhang and Chamseddine (2012). In addition, quadrotors possess simple mechanical structure Alexis et al. (2011), good maneuverability Castillo et al. (2004) and increased payload Dierks and Jagannathan (2010) compared to conventional helicopters and other aircrafts. Hence they have been widely adopted by numerous commercial entities, universities, research institutes, and the military Liu et al. (2015).

However, the quadrotor is classified as an under-actuated system in view of the fact that only four actuators (rotors) are used to control all six Degrees Of Freedom (DOF). The four actuators directly affect the z-axis translation (altitude) and the rotation about each of the three principal axes, while the two remaining DOFs (translation along the x- and y-axis) are coupled, meaning that they depend directly on the overall orientation of the vehicle (the other four DOFs). Additional quadrotors' strengths include swift maneuverability and increased payload. Their drawbacks include an overall larger craft size and higher energy consumption, which in general mean shorter flying time.

Although quadrotors are widely used, their dynamics are relatively unstable and thus requires a control system to stabilize. As a result, various linear and nonlinear control laws have been developed and tested out on quadrotors. A fully autonomous control of a quadrotor poses challenges to control system designers. Some nonlinear control laws that have been studied include the Sliding mode control Xu and Ozguner (2006), and the adaptive Backstepping control Madani and Benallegue (2006). These methods yield very good performance and robustness of the system. However, several practical issues arise when they are applied to the real quadrotor. Besides, several linear control laws such as Proportional Integral Derivative (PID), Linear Quadratic Regulator (LQR) and H_∞ have been studied. However, their performances are limited to

⋆ We would like to express our greatest gratitude toward the late Professor Yasmina BESTAOUI-SEBBANE, Professeure des Universités à l'UFR Sciences et Technologies de l'Université d'Evry-Val-d'Essonne, without whom this project could not have gotten this far.

the hovering condition because the nominal design point of the controller is the hover point. The control of the Unmanned Aerial Vehicle (UAV) can be lost when the UAV departs from the hovering state or undergoes large perturbations. In order to extend the flight maneuverability, a common approach is gain scheduling in which several linear models of the quadrotor are obtained for different trim points. Then the number of Linear Time Invariant (LTI) controllers are derived for each point. As the operating conditions vary, the global controller is estimated by the interpolating gains of the local controllers. Even though this has been successfully implemented in many engineering applications, there is no guarantee for the performance, robustness and nominal stability of the control design Chumalee and Whidborne (2009) Chumalee and Whidborne (2013).

LPV systems are constructed from linear systems which depend on time-varying parameters. They are capable of incorporating many nonlinear and time-varying systems via the so-called quasi-LPV systems in which the parameters are functions of the states and/or inputs of the systems. In LPV systems, convex synthesis conditions, which are extended from Linear Matrix Inequality (LMI)-based LTI control techniques, can be solved by gridding the parameter range. These conditions accept any type of parameter dependence and are especially useful when dealing with non-rational parameter dependence.

In Sadeghzadeh et al. (2014), two different LPV control structures have been synthesized. In the first structure, the H_∞ self-Gain-Scheduling control technique is used to obtain the LPV controller, and the composite quadratic Lyapunov function and quadratic cost function are used to find the optimal state feedback gain. In Rangajeeva and Whidborne (2011), the LPV representation of the quadcopter dynamic has been transformed into a convex polytopic form using Tensor Product transformation. The H_∞ self-Gain-Scheduling control method has been applied to obtain a LPV controller which is tested on a simplified nonlinear model of the quadcopter. However, in these studies, the mass of the quadcopter does not vary in time. In Liu et al. (2017), the authors present an active fault-tolerant control strategy with applications to unmanned quadcopter helicopters. The payload grasping and battery drainage are considered as time-varying parameters. However, the variation of the moments of inertia with respect to the variation of the quadcopter's mass is not considered.

In some of the most recent important applications of UAVs include fetching life jackets, medicines to people in distress, or pesticides to plants in precision agriculture. The mass of the UAVs will change over time (abruptly or gradually). Accordingly, some of the dynamic parameters of the UAV also change wrt the moments of inertia in three axes. This leads to UAV instability.

In our problem, the variation of the mass and the moments of inertia of the UAV will be considered. Therefore, the LPV controller will be selected for controlling the UAV to track the predefined trajectory. A cascaded structure is used to control the quadcopter. First, the attitude is stabilized with robustness against external signals by two LPV H_∞ controllers. The first LPV H_∞ controller is used to control the roll and pitch angles. The other is used to control the yaw angle. The translational subsystem is controlled by a combination of Backstepping and PD controllers.

The proposed cascaded control system is depicted in Fig. (1).

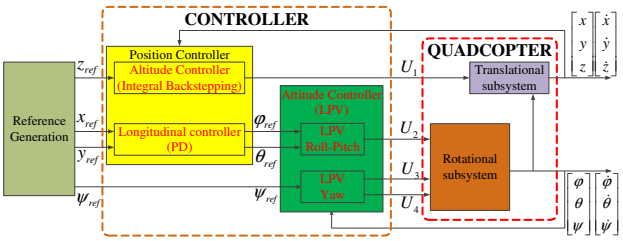

Fig. 1. Control architecture.

The rest of the paper is structured as follows. Section 2 describes the quadcopter system. Section 3 presents the calculation of moments of inertia with respect to the variation of the mass. In section 4, the Backstepping and PD controllers will be used for position controller design. Section 5 shows the design of LPV controller for the attitude of the quadcopter. This LPV controller is the combination of two LPV H_∞ controllers for Roll-Pitch and Yaw subsystems. Section 6 is dedicated for describing the simulation results. Several trajectories and variations of the mass and moments of inertia will be used. The last section concludes and provides directions for further research.

2. DYNAMIC MODEL OF QUADCOPTER

A quadcopter is a four rotor helicopter. It consists of a body fixed frame and four rotors which generate four independent thrusts. The pair of rotors (M_1, M_3) revolve at angular speeds ω_1 and ω_2 in clockwise (CW) direction generating thrusts of τ_1 and τ_3, while the pair of rotors (M_2, M_4) rotates at angular speeds ω_2 and ω_4 in counter-clockwise (CCW) direction generating thrusts of τ_2 and τ_4 (Fig. 2).

By varying the rotor speeds, we can change the lift forces and create motion.

The mathematical model of the quadcopter was generated by the techniques of both Euler-Newton (Bouabdallah, 2007) and Euler-Lagrange (Bouabdallah and Siegwart, 2007).

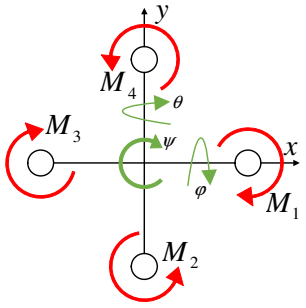

Fig. 2. Quadcopter structure

The quadcopter model is:

$$f(X,U)=\begin{cases}\ddot{x}=(\sin\psi\sin\varphi+\cos\psi\sin\theta\cos\varphi)\dfrac{U_1}{m}\\ \ddot{y}=(\sin\psi\sin\theta\cos\varphi-\cos\psi\sin\varphi)\dfrac{U_1}{m}\\ \ddot{z}=(\cos\theta\cos\varphi)\dfrac{U_1}{m}-g\\ \ddot{\varphi}=\dfrac{I_y-I_z}{I_x}\dot{\theta}\dot{\psi}-\dfrac{J_r\Omega_r}{I_x}\dot{\theta}+\dfrac{l}{I_x}U_2\\ \ddot{\theta}=\dfrac{I_z-I_x}{I_y}\dot{\varphi}\dot{\psi}+\dfrac{J_r\Omega_r}{I_y}\dot{\varphi}+\dfrac{l}{I_y}U_3\\ \ddot{\psi}=\dfrac{I_x-I_y}{I_z}\dot{\varphi}\dot{\theta}+\dfrac{1}{I_z}U_4\end{cases}\quad(1)$$

where (x,y,z) are the three positions, (φ,θ,ψ) are the three Euler angles. The other parameters are shown below.

The quadcopter's inputs are: the thrust force (U_1) and three torques (roll torque (U_2), pitch torque (U_3), and yaw torque (U_4)), the force and torques are related on the rotor speed:

$$\begin{cases}U_1=b\left(\omega_1^2+\omega_2^2+\omega_3^2+\omega_4^2\right)\\ U_2=b\left(\omega_4^2-\omega_2^2\right)\\ U_3=b\left(\omega_3^2-\omega_1^2\right)\\ U_4=d\left(\omega_1^2-\omega_2^2+\omega_3^2-\omega_4^2\right)\end{cases}\quad(2)$$

$$\Omega_r=\omega_1-\omega_2+\omega_3-\omega_4\quad(3)$$

Where $\omega_i, i=1,..,4$ are angular velocity of the i_{th} rotor, Ω_r is the overall residual propeller angular speed, b and d are thrust and drag coefficients.

All quadcopter parameters for simulation (Fig. 1), are taken from (Bouabdallah, 2007) below.

Table 1. Quadcopter parameters definition

Parameter	Name	Value	Unit
m	Quadcopter mass	0.65	Kg
l	Arm length	0.23	m
b	Thrust coefficient	$3.13x10^5$	$N\cdot m^2$
d	Drag coefficient	7.5×10^{-7}	$N\cdot m\cdot s^2$
I_x, I_y	Inertia on x and y axis	7.5×10^{-3}	$Kg\cdot m^2$
I_z	Inertia on z axis	1.3×10^{-2}	$Kg\cdot m^2$
J_r	Rotor inertia	6×10^{-5}	$Kg\cdot m^2$
ω_i	Rotor speed	$[0,400]$	$rad\cdot s^{-1}$

Suppose that the quadcopter is symmetric, which means that $I_x=I_y$. Consequently, a simplified mathematical model of the quadcopter can be rewritten as follows:

$$f(X,U)=\begin{cases}\ddot{x}=(\sin\psi\sin\varphi+\cos\psi\sin\theta\cos\varphi)\dfrac{U_1}{m}\\ \ddot{y}=(\sin\psi\sin\theta\cos\varphi-\cos\psi\sin\varphi)\dfrac{U_1}{m}\\ \ddot{z}=(\cos\theta\cos\varphi)\dfrac{U_1}{m}-g\\ \ddot{\varphi}=\dfrac{I_x-I_z}{I_x}\dot{\theta}\dot{\psi}+\dfrac{l}{I_x}U_2\\ \ddot{\theta}=\dfrac{I_z-I_x}{I_x}\dot{\varphi}\dot{\psi}+\dfrac{l}{I_x}U_3\\ \ddot{\psi}=\dfrac{1}{I_z}U_4\end{cases}\quad(4)$$

3. CALCULATION OF MOMENTS OF INERTIA

When the UAV sprays pesticides or delivers packages, the mass of the UAV decreases gradually or abruptly. In both cases, the total mass of the UAV is the same and is divided into several cylinders. Nevertheless in the case of a gradual mass reduction, the number of cylinders is much larger than the case of a sudden mass change. In particular, we assume that there are n cylinders $m_1, m_2, ..., m_n$ attached to the UAV as shown in Fig. 3. Each cylinder $m_i, i=1,...,n$ has the height h_i, radius r, and mass m_i. To simulate the process of reducing the mass of the UAV, the cylinders $m_i, i=1,...,m$ will be sequentially $(m_n,...,m_1)$ detached from the UAV over time. We call x_k, y_k, and z_k (Fig. 3) are the three axes x, y, and z for calculation the moments of inertia of the mass which contains k cylinders from 1 to k, where $k=1,...,n$.

Due to the variation of the mass of the UAV over time, the moments of inertia will also change. Therefore, the moments of inertia of the whole system need to be recalculated at each change.

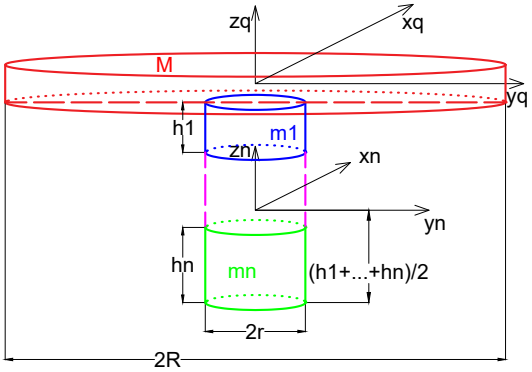

Fig. 3. Moment of inertia of the systems quadcopter-mass

Moments of inertia of mass $(m_1+...+m_k), k=1,...,n$ with respected to their x and y axes x_k and y_k respectively are:

$$J_{(m_1+...+m_k)/x_k}=J_{(m_1+...+m_k)/y_k}=\left(\sum_{i=1}^{k}m_i\right)\frac{r^2}{4}+\left(\sum_{i=1}^{k}m_i\right)\frac{\left(\sum_{i=1}^{k}h_i\right)^2}{12}$$

Hence, moments of inertia of mass $(m_1+...+m_k), k=1,...,n$ with respected to the axes x_q and y_q of the quadcopter are:

$$J_{(m_1+...+m_k)/x_q}=J_{(m_1+...+m_k)/y_q}=J_{(m_1+...+m_k)/x_k}+\left(\sum_{i=1}^{k}m_i\right)\frac{\left(\sum_{i=1}^{k}h_i\right)^2}{2}=\sum_{i=1}^{n}m_i\left(\frac{r^2}{4}+\frac{7}{12}\left(\sum_{i=1}^{k}h_i\right)^2\right)$$

Moments of inertia of mass $(m_1+...+m_k), k=1,...,n$ with respected to their z_k axes and the z_q axis of the quadcopter are:

$$J_{(m_1+...+m_k)/z_k}=J_{(m_1+...+m_k)/z_q}=\left(\sum_{i=1}^{k}m_i\right)\frac{r^2}{2}$$

Finally, moments of inertia of system which contains the quadcopter and k cylinders $m_1, ..., m_k, k = 1, .., n$ with respected to the three axis of the quadcopter x_q, y_q, and z_q are:

$$\begin{aligned} J_{[quad\_(m_1+...+m_k)]/x_q} &= J_{quad/x_q} + J_{(m_1+...+m_k)/x_q} \\ &= J_{quad/x_q} + \sum_{i=1}^{k} m_i \left(\frac{r^2}{4} + \frac{7}{12} \left(\sum_{i=1}^{k} h_i \right)^2 \right) \end{aligned}$$

$$\begin{aligned} J_{[quad\_(m_1+...+m_k)]/y_q} &= J_{quad/y_q} + J_{(m_1+...+m_k)/y_q} \\ &= J_{quad/y_q} + \sum_{i=1}^{k} m_i \left(\frac{r^2}{4} + \frac{7}{12} \left(\sum_{i=1}^{k} h_i \right)^2 \right) \end{aligned}$$

$$\begin{aligned} J_{[quad\_(m_1+...+m_k)]/z_q} &= J_{quad/z_q} + J_{(m_1+...+m_k)/z_q} \\ &= J_{quad/z_q} + \left(\sum_{i=1}^{k} m_i \right) \frac{r^2}{2} \end{aligned}$$

4. POSITION CONTROL

In this section, the translational subsystem will be considered. The differential equations of dynamic translational subsystem is as:

$$\begin{cases} \ddot{x} = (\sin\psi \sin\varphi + \cos\psi \sin\theta \cos\varphi) \dfrac{U_1}{m} \\ \ddot{y} = (\sin\psi \sin\theta \cos\varphi - \cos\psi \sin\varphi) \dfrac{U_1}{m} \\ \ddot{z} = (\cos\theta \cos\varphi) \dfrac{U_1}{m} - g \end{cases} \tag{5}$$

State vector is

$$X = [\, x \;\; \dot{x} \;\; y \;\; \dot{y} \;\; z \;\; \dot{z} \,]^T = [\, x_1 \;\; x_2 \;\; x_3 \;\; x_4 \;\; x_5 \;\; x_6 \,]^T$$

4.1 Altitude control

In this subsection, altitude controller is designed to track the reference. The error of the third state x_5, its derivative and integral are defined as follows:

$$\begin{aligned} z_5 &= x_{5d} - x_5 \\ \dot{z}_5 &= \dot{x}_{5d} - x_6 \\ \xi_5 &= \int_0^t z_5(\tau)\, d\tau \end{aligned} \tag{6}$$

The Lyapunov function and its derivative are:

$$\begin{aligned} V(z_5) &= \frac{1}{2} z_5^2 \\ \dot{V}(z_5) &= z_5 (\dot{x}_{5d} - x_6) \end{aligned} \tag{7}$$

We can see no direct control law in (7). Consequently, x_6 is defined as a virtual control. To make $\dot{V}(z_5)$ negative semi-definite, the desired virtual control is defined as:

$$x_{6d} = \dot{x}_{5d} + c_5 z_5 + \lambda_5 \xi_5 \tag{8}$$

where c_5 and λ_5 are positive numbers.

In order to make x_6 follows the stabilizing function x_{6d}, we define the error state z_6 as the deviation between x_{6d} and x_6:

$$z_6 = x_{6d} - x_6 \tag{9}$$

The virtual control x_6 and the derivative of z_6 are:

$$x_6 = \dot{x}_{5d} + c_5 z_5 + \lambda_5 \xi_5 - z_6 \tag{10}$$

$$\dot{z}_6 = \ddot{x}_{5d} + c_1 \dot{z}_5 + \lambda_5 \xi_5 - \frac{\cos\varphi \cos\theta}{m} U_1 + g \tag{11}$$

The Lyapunov function is extended by z_5 and ξ_5:

$$V_1 = \frac{1}{2} z_5^2 + \frac{1}{2} \lambda_5 \xi_1^2 \tag{12}$$

The derivative of the Lyapunov function is:

$$\begin{aligned} \dot{V}_1 &= z_5 \dot{z}_5 + \lambda_5 \xi_1 \dot{\xi}_1 \\ &= z_5 (\dot{x}_{5d} - x_6) + \lambda_5 \xi_5 z_5 \\ &= z_5 (z_6 - c_5 z_5 - \lambda_5 \xi_5) + \lambda_5 \zeta_5 z_5 \\ &= -c_5 z_5^2 + z_5 z_6 \end{aligned} \tag{13}$$

For making the derivative of Lyapunov function negative, z_5 should be added to it:

$$V_2 = \frac{1}{2} z_5^2 + \frac{1}{2} \lambda_5 \xi_1^2 + \frac{1}{2} z_5^2 \tag{14}$$

$$\begin{aligned} &\dot{V}_2 = -c_5 z_5^2 + z_5 z_6 \\ &+ z_5 \left(\ddot{x}_{5d} + c_1 \dot{z}_5 + \lambda_5 \xi_5 - \frac{\cos\varphi \cos\theta}{m} U_1 + g \right) \end{aligned} \tag{15}$$

$$\begin{aligned} &U_1 = \frac{m}{\cos\varphi \cos\theta} \\ &\left(\ddot{x}_{5d} + \left(1 - c_5^2 + \lambda_5\right) z_5 - c_5 \lambda_5 \xi_5 + (c_5 + c_6) z_6 + g \right) \end{aligned} \tag{16}$$

$$\dot{V}_2 = -c_5 z_5^2 - c_6 z_6^2 \tag{17}$$

Coefficients of Back-stepping controller are selected as:

$$c_8 = 0.001; \qquad c_7 = 30; \qquad \lambda_5 = 30$$

4.2 Longitudinal control

As U_1 controls z, we can only define desired φ_d and θ_d to be computed to achieve that x_c and y_c go to desired x_d and y_d.

In this subsection, a simple PD controller is designed for calculating the required roll φ_d and pitch θ_d.

We define the position and velocity errors x and y as:

$$\begin{aligned} e_{px} &= x_d - x, \quad & e_{vx} &= \dot{x}_d - \dot{x} \\ e_{py} &= y_d - y, \quad & e_{vy} &= \dot{y}_d - \dot{y} \end{aligned}$$

And we want these errors to decay exponentially to 0.

If we take the error term and make it obey a second order linear differential equation with proper coefficients, we can guarantee that the error goes exponentially to 0.

Means:

$$\begin{aligned} \ddot{x}_d - \ddot{x}_c + K_{dx} \dot{e}_{vx} + K_{px} e_{px} = 0 \\ \ddot{y}_c - \ddot{y}_c + K_{dy} \dot{e}_{vy} + K_{py} e_{py} = 0 \end{aligned}$$

where $\ddot{x}_c$ and $\ddot{y}_c$ are the commanded accelerations which are calculated by the controller.

Hence, the second derivative of commanded x_c and y_c are calculated as:

$$\begin{cases} \ddot{x}_c = \ddot{x}_d + K_{p_x} (x_d - x) + K_{d_x} (\dot{x}_d - \dot{x}) \\ \ddot{y}_c = \ddot{y}_d + K_{p_y} (y_d - y) + K_{d_y} (\dot{y}_d - \dot{y}) \end{cases} \tag{18}$$

Suppose that the quadcopter is around the hover position, we have:

$$U_1 \sim mg, \theta \sim 0, \varphi \sim 0, \psi \sim \psi_d$$

Therefore, the required φ_d and θ_d can be obtained as:

$$\begin{cases} \varphi_d = \dfrac{1}{g}\left(\ddot{x}_c \cdot \sin\psi_d - \ddot{y}_c \cdot \cos\psi_d\right) \\ \theta_d = \dfrac{1}{g}\left(\ddot{x}_c \cdot \cos\psi_d + \ddot{y}_c \cdot \cos\psi_d\right) \end{cases} \tag{19}$$

Coefficients of PD controller are selected as:

$$K_{P_x} = 20; \quad K_{d_x} = 2; \quad K_{P_y} = 25; \quad K_{d_y} = 3$$

5. LPV H_∞ ATTITUDE CONTROL

In this section, the rotational subsystem will be considered. The differential equations of dynamic rotational subsystem is as:

$$\begin{cases} \ddot{\varphi} = \dfrac{I_x - I_z}{I_x}\dot{\theta}\dot{\psi} + \dfrac{l}{I_x}U_2 \\ \ddot{\theta} = \dfrac{I_z - I_x}{I_x}\dot{\varphi}\dot{\psi} + \dfrac{l}{I_x}U_3 \\ \ddot{\psi} = \dfrac{1}{I_z}U_4 \end{cases} \tag{20}$$

Roll-pitch H_∞ controller The dynamic of Roll-Pitch subsystem is rewritten in descriptor form for reducing the number of subsystems and have linear parameters as

$$\begin{cases} I_x\ddot{\varphi} = \left(I_x - I_z\right)\dot{\theta}\dot{\psi} - J_r\Omega_r\dot{\theta} + lU_2 \\ I_x\ddot{\theta} = -\left(I_x - I_z\right)\dot{\varphi}\dot{\psi} + J_r\Omega_r\dot{\varphi} + lU_3 \end{cases} \tag{21}$$

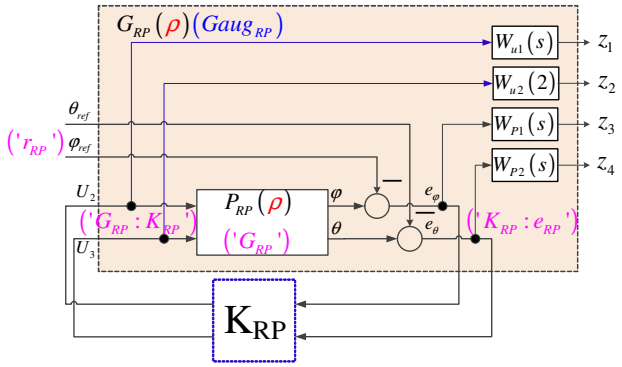

Fig. 4. Roll Pitch H_∞ controller.

State vector is

$$X_{RP}^T = \left[\varphi \;\; \theta \;\; \dot{\varphi} \;\; \dot{\theta}\right]^T$$

The roll-pitch susbsystem can be written as:

$$\begin{aligned} E_{RP}\dot{X} &= A_{RP}X + B_{RP}u \\ y &= C_{RP}X + D_{RP}u \end{aligned} \tag{22}$$

where:

$$E_{RP} = \begin{bmatrix} 1 & 0 & 0 & 0 \\ 0 & 1 & 0 & 0 \\ 0 & -\left(I_x - I_z\right)\dot{\psi} + J_r\Omega_r & I_x & 0 \\ -\left(I_x - I_z\right)\dot{\psi} - J_r\Omega_r & 0 & 0 & I_y \end{bmatrix}$$

$$A_{RP} = \begin{bmatrix} 0 & 0 & 1 & 0 \\ 0 & 0 & 0 & 1 \\ 0 & 0 & 0 & 0 \\ 0 & 0 & 0 & 0 \end{bmatrix}; \quad B_{RP} = \begin{bmatrix} 0 & 0 \\ 0 & 0 \\ l & 0 \\ 0 & l \end{bmatrix}$$

$$C_{RP} = \begin{bmatrix} 1 & 0 & 0 & 0 \\ 0 & 1 & 0 & 0 \end{bmatrix}; \quad D_{RP} = \begin{bmatrix} 0 & 0 \\ 0 & 0 \end{bmatrix}$$

The parameter ρ_{RP} that is varying is:

$$\begin{aligned} \rho_{RP} &= \left[\, I_x \;\; \left(I_x - I_z\right)\dot{\psi} \;\; \Omega_r \,\right]^T \\ &= \left[\, \rho_{RP1} \;\; \rho_{RP2} \;\; \rho_{RP3} \,\right]^T \end{aligned}$$

Their varying ranges are in table 2.

Table 2. Parameters range for LPV H_∞ Roll-Pitch and Yaw controllers

Parameter	Description	Range
ρ_{RP_1}	I_x	$[0.0075, 0.0128]\, kg.m^2$
ρ_{RP_2}	$\left(I_x - I_z\right)\dot{\psi}$	$\left[-5 \times 10^{-4}, 0.0173\right]\, kg.m^2$
ρ_{RP_3}	Ω_r	$[-300, 300]\, rad.s^{-1}$
ρ_Y	I_z	$[0.0130, 0.0162]\, kg.m^2$

In order to express the system in polytopic form, matrices $A_{RP}, B_{RP}, C_{RP}, D_{RP}, E_{RP}$ can be decomposed as:

$$\begin{aligned} A_{RP} &= A_{RP_0} + \rho_{RP_1}A_{RP_1} + \rho_{RP_2}A_{RP_2} + \rho_{RP_3}A_{RP_3} \\ B_{RP} &= B_{RP_0} + \rho_{RP_1}B_{RP_1} + \rho_{RP_2}B_{RP_2} + \rho_{RP_3}B_{RP_3} \\ C_{RP} &= C_{RP_0} + \rho_{RP_1}C_{RP_1} + \rho_{RP_2}C_{RP_2} + \rho_{RP_3}C_{RP_3} \\ D_{RP} &= D_{RP_0} + \rho_{RP_1}D_{RP_1} + \rho_{RP_2}D_{RP_2} + \rho_{RP_3}D_{RP_3} \\ E_{RP} &= E_{RP_0} + \rho_{RP_1}E_{RP_1} + \rho_{RP_2}E_{RP_2} + \rho_{RP_3}E_{RP_3} \end{aligned}$$

where:

$$A_0 = \left[\begin{array}{c|c} 0_2 & I_{22} \\ \hline 0_{22} & 0_{22} \end{array}\right]; A_1 = A_2 = A_3 = A_4 = [0_{44}]$$

$$B_0 = l\left[\begin{array}{c} 0_{22} \\ \hline I_{22} \end{array}\right]; B_1 = B_2 = B_3 = B_4 = [0_{42}]$$

$$C_0 = \left[\, I_{22} \middle| 0_{22} \,\right]; C_1 = C_2 = C_3 = C_4 = [0_{24}]$$

$$D_0 = D_1 = D_2 = D_3 = D_4 = [0_{22}]$$

$$E_0 = \begin{bmatrix} I_{22} & 0_{22} \\ 0_{22} & 0_{22} \end{bmatrix}; E_1 = \begin{bmatrix} 0_{22} & 0_{22} \\ 0_{22} & I_{22} \end{bmatrix};$$

$$E_2 = \begin{bmatrix} 0_{22} & 0_{22} \\ 0 & -1 \\ 1 & 0 \end{bmatrix}; E_3 = \begin{bmatrix} 0_{22} & 0_{22} \\ 0 & -J_r \\ J_r & 0 \end{bmatrix}$$

Weight functions for Roll-Pitch H_∞ controller are chosen as following:

$$W_{u1} = \frac{s}{s + 400000}; W_{u2} = \frac{s}{s + 400000}$$
$$W_{P1} = \frac{1}{s + 0.1}; W_{P2} = \frac{1}{s + 0.1}$$

The norm of LPV H_∞ Roll-Pitch subsystem is $\gamma_{RP} = 0.544$

Yaw H_∞ controller The dynamic of Yaw susbsystem is rewritten in descriptor form as

$$I_z\ddot{\psi} = U_4 \tag{23}$$

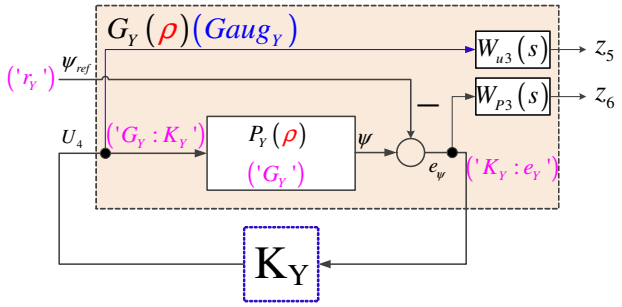

Fig. 5. Yaw H_∞ controller.

State vector is $X_Y^T = \begin{bmatrix} \psi & \dot{\psi} \end{bmatrix}^T$

The roll-pitch susbsystem can be written as:

$$\begin{aligned} E_Y \dot{X}_Y &= A_Y X + B_Y u_Y \\ y_Y &= C_Y X + D_Y u_Y \end{aligned} \tag{24}$$

where:

$$A_Y = \begin{bmatrix} 0 & 1 \\ 0 & 0 \end{bmatrix}; \quad B_Y = \begin{bmatrix} 0 \\ 1 \end{bmatrix}; \quad C_Y = \begin{bmatrix} 1 & 0 \end{bmatrix};$$
$$D_Y = [0]; \quad E_Y = \begin{bmatrix} 1 & 0 \\ 0 & I_z \end{bmatrix}$$

The parameter ρ_Y that is varying is: $\rho_Y = [I_z]$. Its varying range is in table 2.

In order to express the system in polytopic form, matrices A_Y, B_Y, C_Y, D_Y, E_Y can be decomposed as:

$$\begin{aligned} A_Y &= A_{Y_0} + \rho_Y A_{Y_1} \\ B_Y &= B_{Y_0} + \rho_Y B_{Y_1} \\ C_Y &= C_{Y_0} + \rho_Y C_{Y_1} \\ D_Y &= D_{Y_0} + \rho_Y D_{Y_1} \\ E_Y &= E_{Y_0} + \rho_Y E_{Y_1} \end{aligned}$$

where:

$$A_{Y_0} = \begin{bmatrix} 0 & 1 \\ 0 & 0 \end{bmatrix}; A_{Y_1} = \begin{bmatrix} 0 & 0 \\ 0 & 0 \end{bmatrix}; B_{Y_0} = \begin{bmatrix} 0 \\ 1 \end{bmatrix}; B_{Y_1} = \begin{bmatrix} 0 \\ 0 \end{bmatrix}$$
$$C_{Y_0} = \begin{bmatrix} 1 & 0 \end{bmatrix}; \; C_{Y_1} = \begin{bmatrix} 0 & 0 \end{bmatrix}; \; D_{Y_0} = [0]; D_{Y_1}\,[0]$$
$$E_{Y_0} = \begin{bmatrix} 1 & 0 \\ 0 & 0 \end{bmatrix}; \; E_{Y1} = \begin{bmatrix} 0 & 0 \\ 0 & 1 \end{bmatrix}$$

Weight functions for Yaw H_∞ controller are chosen as following:

$$W_{u3} = \frac{0.25}{s + 0.2}$$
$$W_{P3} = \frac{s^3 + 0.03s^2}{s^3 + 12000s^2 + 11300000s + 1000}$$

The norm of LPV H_∞ Yaw subsystem is $\gamma_Y = 0.0188$

6. SIMULATION AND RESULT'S COMMENTS

In this section, we propose the trajectory: first, the quadcopter goes up $2m$ on altitude, and then follows a square of $8m$ of side on x and y (Fig. 13). The yaw angle ψ is not change during the flight.

The mass declines in two manners: gradually and abruptly. A test for the robustness of the proposed controller with respect to step and impulse disturbances is also considered. In particular, we consider wind as a source of disturbances.

The first type of disturbances involves a series of wind impulses with velocity $V_w = 7\cdot\mathbf{i}+7\cdot\mathbf{j}+7\cdot\mathbf{k}$ at $5s$, $15s$, $25s$, $35s$, $45s$, $55s$, $65s$, $75s$, $85s$, respectively. The second type of disturbances comes from two wind steps with velocity $V_w = 1\cdot\mathbf{i}+1\cdot\mathbf{j}+1\cdot\mathbf{k}$ from $15s$ to $25s$, and from $55s$ to $65s$, respectively. Both types of disturbances are demonstrated in the fourth plot of Fig. (6) . In this figure, the changes of mass, moments of inertia wrt to the three axis x, y, z are shown in the first, second, and third plot, respectively.

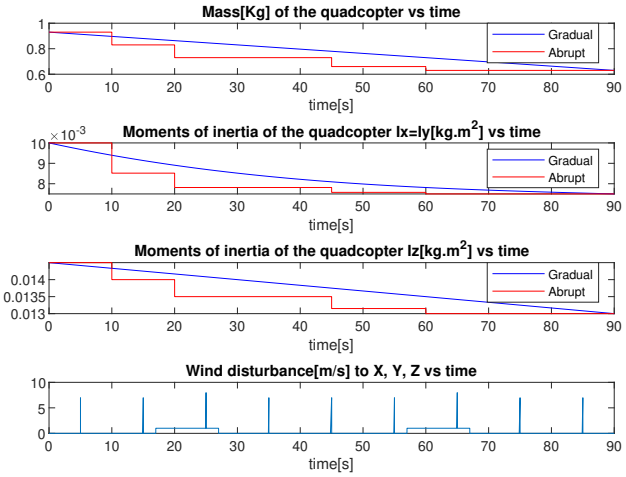

Fig. 6. Variation of mass and moments of inertia and disturbances.

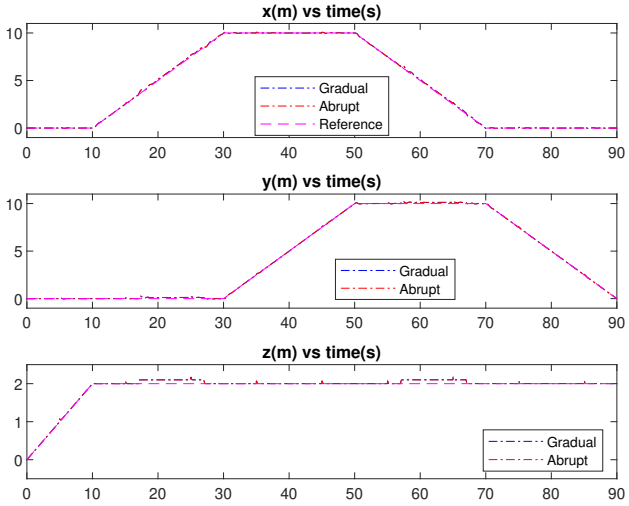

Fig. 7. Translation coordinates: X, Y, Z.

In the gradual mass reduction simulation, the mass reduces gradually from $0.93\,[kg]$ to $0.6\,[kg]$) in a period from $0s$ to $90s$, as shown in the first plot of Fig. (6). At each point the mass changes, the recalculated moments of inertia are shown in the second and third plots of the same figure.

In the abrupt mass reduction simulation, the mass declines abruptly at $10s$ (from $0.93\,[kg]$ to $0.83\,[kg]$), at $20s$ (from $0.83\,[kg]$ to $0.73\,[kg]$), at $45s$ (from $0.73\,[kg]$ to $0.63\,[kg]$), and at $60s$ (from $0.63\,[kg]$ to $0.6\,[kg]$), as shown in the first plot of Fig. (6). At each point the mass changes, the recalculated moments of inertia are shown in the second and third plots of the same figure.

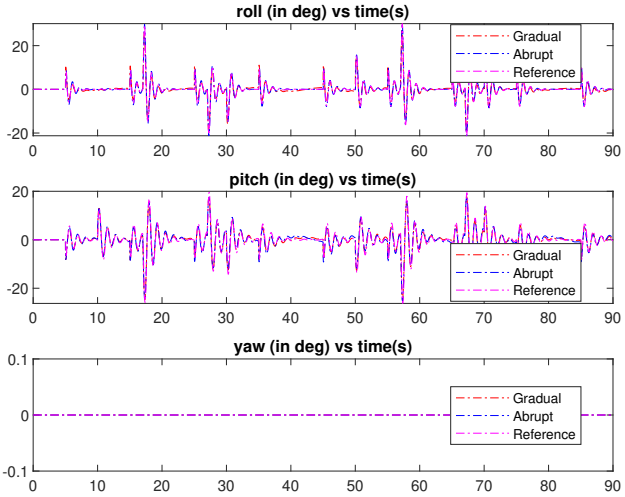

Fig. 8. Orientation coordinates: φ, θ, ψ.

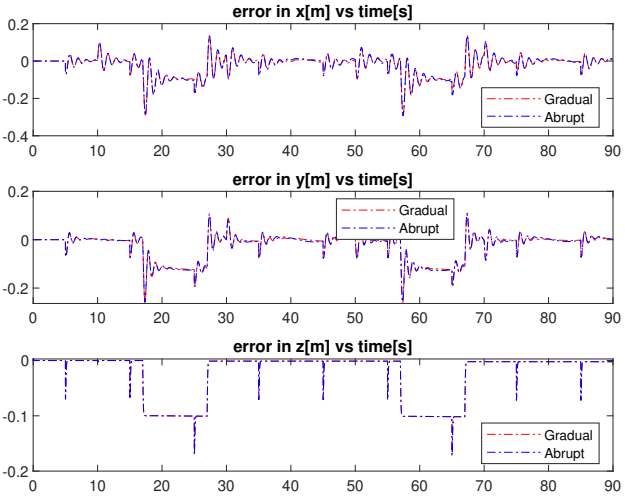

Fig. 9. Error in X, Y, Z, ψ.

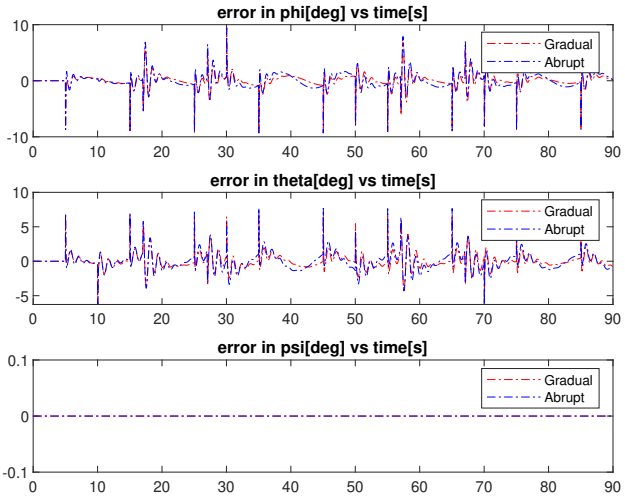

Fig. 10. Error in ϕ, θ, and ψ.

Comments on simulation results

From the simulation results, we can see that the quadcopter is stable and tracks the predefined trajectory well under the variation of dynamic parameters and the presence of disturbances.

Fig. (8) shows that the roll, pitch and yaw angles track their designated trajectories. The error of roll, pitch and

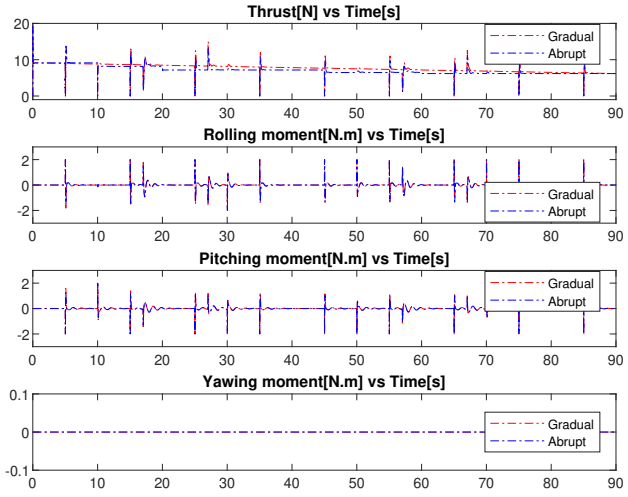

Fig. 11. Input signals: U_1, U_2, U_3, U_4.

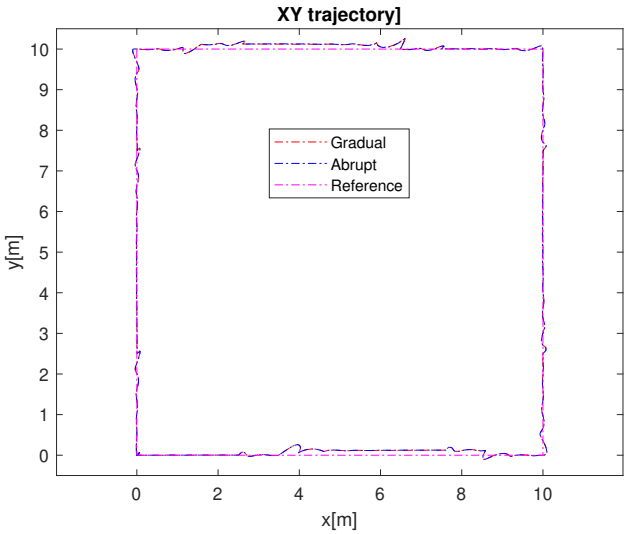

Fig. 12. Horizontal trajectory.

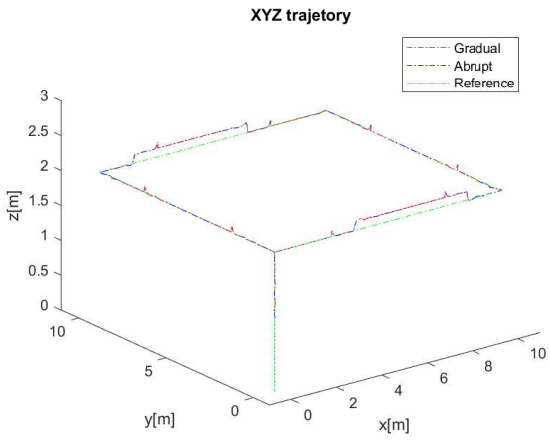

Fig. 13. 3D trajectory.

yaw are shown in Fig. (10). The maximum error is about 10 degrees only at the very moment of disturbances, but it quickly drops to near 0 degree.

Fig. (7) shows the references and responses in x, y, and z. Fig. (9) shows the errors wrt to x, y, and z and ψ.

In both instances of mass variation, the quadcopter still tracks the predefined trajectory even under step and impulse disturbances, as shown in Fig. (12) and Fig. (13).

CONCLUSION

In this paper, we have proposed a robust controller for the quadcopter with time-varying mass. This controller contains the LPV-H_∞ for the inner loop and a combination of integral Backstepping and PD controllers for the outer loop. The results show that the controller are robust to the manner of mass variation, as well as to step and impulse disturbances.

For simplicity we have assumed that the quadcopter is symmetric, meaning that $I_x = I_y$. Several extensions from this research are possible. One might consider a non symmetric structure, a different control technique, or the implementation of experiments on a real quadcopter platform to verify the simulation results presented in this study.

REFERENCES

Kostas Alexis, George Nikolakopoulos, and Anthony Tzes. Switching model predictive attitude control for a quadrotor helicopter subject to atmospheric disturbances. *Control Engineering Practice*, 19:1195–1207, 2011. doi: 10.1016/j.conengprac.2011.06.010.

Samir Bouabdallah. Design and control of quadrotors with application to autonomous flying. 01 2007. doi: 10.5075/epfl-thesis-3727.

Samir Bouabdallah and Roland Siegwart. Backstepping and Sliding-mode Techniques Applied to an Indoor Micro Quadrotor. *Intelligent Robots and Systems, 2007. IROS 2007. IEEE/RSJ International Conference*, pages 153–158, 2007.

Pedro Castillo, Alejandro Dzul, and Rogelio Lozano. Real-time stabilization and tracking of a four-rotor mini rotorcraft. *Control Engineering Practice*, 12(4):510 – 516, 2004. doi: 10.1109/TCST.2004.825052.

Sunan Chumalee and James F Whidborne. Gain-scheduled H_∞ autopilot design via parameter dependent lyapunov functions. *AIAA Guidance, Navigation and Control Conference*, 2009. doi: 10.1080/00207721.2013.775386.

Sunan Chumalee and James F Whidborne. Gain-scheduled H_∞ control via parameter-dependent lyapunov functions. *International Journal of Systems Science*, pages 1 – 14, 2013. doi: 10.1080/00207721.2013.775386.

Travis Dierks and Sarangapani Jagannathan. Output feedback control of a quadrotor uav using neural networks. *IEEE Transactions on Neural Networks*, 21(1):50 – 66, 2010. doi: 10.1109/TNN.2009.2034145.

Zhixiang Liu, Chi Yuan, Youmin Zhang, and Jun Luo. A learning-based fault tolerant tracking control of an unmanned quadrotor helicopter. *Journal of Intelligent and Robotic Systems*, 84(1-4):145–162, 2015. doi: 10.1007/s10846-015-0293-0.

Zhixiang Liu, Chi Yuan, and Youmin Zhang. Active fault-tolerant control of unmanned quadrotor helicopter using linear parameter varying technique. *J Intell Robot Syst*, 88:415–436, 2017. doi: 10.1007/s10846-017-0535-4.

Tarek Madani and Abdelaziz Benallegue. Control of a quadrotor mini-helicopter via full state backstepping technique. *45th IEEE Conference on Decision and Control*, pages 1515–1520, 2006. doi: 10.1109/CDC.2006.377548.

Samarathunga L.M.D. Rangajeeva and James F. Whidborne. Linear parameter varying control of a quadrotor. *2011 6th International Conference on Industrial and Information Systems, ICIIS*, page 483–488, 2011.

Iman Sadeghzadeh, Abbas Chamseddine, Didier Theilloiol, and Youmin Zhang. Linear parameter varying control synthesis: State feedback versus H_∞ technique with application to quadrotor uav. *2014 International Conference on Unmanned Aircraft Systems (ICUAS) May 27-30, 2014. Orlando, FL, USA*, pages 1099 – 1104, 2014.

Rong Xu and Umit Ozguner. Sliding mode control of a quadrotor helicopter. *45th IEEE Conference on Decision and Control*, pages 4957–4962, 2006. doi: 10.1109/CDC.2006.377588.

Youmin Zhang and Abbas Chamseddine, editors. *Fault tolerant flight control techniques with application to a quadrotor UAV testbed*. INTECH Open Access Publisher, 2012. doi: DOI: 10.5772/38918.